Available online at http://scik.org
Commun. Math. Biol. Neurosci. 2023, 2023:26
https://doi.org/10.28919/cmbn/7795
ISSN: 2052-2541

STABILITY ANALYSIS OF A NONLINEAR MATHEMATICAL MODEL FOR COVID-19 TRANSMISSION DYNAMICS

PADMA BHUSHAN BORAH[1], BHAGYA JYOTI NATH[2,*], KUMUD CHANDRA NATH[3], HEMANTA KUMAR SARMAH[1]

[1]Department of Mathematics, Gauhati University, Guwahati 781014, Assam, India

[2]Department of Mathematics, Barnagar College, Sorbhog 781317, Assam, India

[3]Department of Mathematics, Dispur College, Guwahati 781006, Assam, India

Abstract. The whole world had been plagued by the COVID-19 pandemic. It was first detected in the Wuhan city of China in December 2019, and has then spread worldwide. It has affected each one of us in the worst possible way. In the current study, a differential equation-based mathematical model is proposed. The present model highlights the infection dynamics of the COVID-19 spread taking hospitalization into account. The basic reproduction number is calculated. This is a crucial indicator of the outcome of the COVID-19 dynamics. Local stability of the equilibrium points has been studied. Global stability of the model is proven using the Lyapunov second method and the LaSalle invariance principle. Sensitivity analysis of the model is performed to distinguish the factor responsible for the faster spread of the infection. Finally, the theoretical aspects have been corroborated via numerical simulations performed for various initial conditions and different values of the parameters.

Keywords: mathematical modeling; basic reproduction number; global stability; Lyapunov function; sensitivity analysis; COVID-19 disease.

2020 AMS Subject Classification: 92-10, 92D30, 34D05, 34D20, 34D23.

*Corresponding author

E-mail address: bhagyajyotinath13@gmail.com

Received October 21, 2022

1. INTRODUCTION

One of the most disastrous pandemics the world has witnessed throughout its history is the COVID-19 epidemic. On March 11, 2020, the World Health Organization (WHO) declared COVID-19 a pandemic. The vast majority of (COVID-19) cases are transmitted through human-to-human contact. The virus is spread through direct contact with an infected individual. There have been more than 600 million cases of COVID-19 infection and more than 6 million deaths worldwide[1, 2, 3]. It is crucial to note that the number of cases is underestimated for a variety of factors, including a lack of diagnostics and asymptomatic cases[4, 5, 6, 7, 8, 9, 10, 11, 12]. The first case of COVID-19 infection was reported in the city of Wuhan, Hubei province of China[13, 14, 15, 16, 17]. Thereafter, the virus spread worldwide, affecting nearly each and every country.

The contribution of epidemiological modelling to the study of infectious disease transmission dynamics has been significant[18, 19, 20, 21, 22]. Modeling the dynamics of smallpox in 1760 marked the beginning of the study of epidemic dynamics, which has since become an essential tool for studying the spread and control of infectious diseases[23]. Kermack and McKendrick presented the the well-known Susceptible-Infected-Removed (SIR) model of ordinary differential equations in their ground-breaking paper[24]. In the 1950s and early 1960s, Bailey [25] and Bartlett [26] developed stochastic theories of disease dynamics. Bartlett also pioneered the application of Monte Carlo simulations to the study of epidemics[28, 27].

Since the emergence of the COVID-19, several writers have contributed to the literature of epidemiological modelling, e.g. see [55, 29, 30, 31, 32, 33, 34, 35, 36, 37, 38, 39, 40, 41, 42, 43, 44, 45, 46, 47, 48, 49, 50, 51, 52, 53, 54]. The classical SIR compartmental model splits the whole population into three compartments: S(t), I(t), and R(t), representing the proportion of the population susceptible to infection, infected individuals, and removed people (recovered or dead), respectively[56]. However, for the majority of infectious diseases, a latent phase precedes the transition from the diseased to the infectious state. This necessitates an additional compartment in the model, namely the exposed population E(t), making it a system of four ODEs.[57]. Effective use of SEIR has been made to comprehend the early dynamics of the COVID-19 outbreak and to assess the efficacy of various actions since the outbreak[58, 59, 60,

61, 62]. In [63], the classical SEIR model was expanded to include delays in order to incorporate the incubation period into the COVID-19 dynamics.

In this work, we extend the SEIR model by considering the class of quarantined individuals $Q(t)$, and those individuals who are under treatment $T(t)$. These classes are not infectious since they are under proper isolation. This is important since deterministic models with fewer compartments such as SIR or SEIR, fail to adequately characterize the evolution of COVID-19, as proved in [64]. Using dynamical system theory, this study aims to analyze the dynamics of the COVID-19 epidemic using the SEIQTR model. The discrete model is equally accurate, but we rely on the continuous deterministic model because it is easier to process. We will first evaluate the local stability of the model under both disease-free and endemic equilibrium conditions, and then we will test the model's global stability.

The rest of this paper is organized as follows. In Section 2, we formulate the mathematical model for the spread of COVID-19 infection, in Section 3, we present some basic properties such as positivity and boundedness of the model. The next section is committed to the derivation of the basic reproduction number. Section 5 is devoted to the stability analysis of the model including both local as well as global stability. Section 6 and 7 contains bifurcation analysis and sensitivity analysis of the basic reproduction number, respectively. In Section 8, we study some numerical simulations of our model substantiating results obtained in the previous sections. The last section is dedicated to discussion and conclusion.

2. Formulation of the Mathematical Model

We construct a compartmental model[65] for the spread of COVID-19 based on a continuous time deterministic nonlinear system of the differential equations. For the purpose of the model, we divide the whole population into six compartments, viz., the compartment of people susceptible to the disease $S(t)$, people exposed to the disease who are not yet infectious $E(t)$, the compartment of infected and infectious people $I(t)$, the quarantined class $Q(t)$, those are under treatment $T(t)$, and the class $R(t)$ of people recovered from COVID-19. Each compartment is assumed to be homogeneous. So all individuals within the same compartment are subject to the same hazards. We assume that once someone is recovered from the disease, she or he becomes

immune. All newborns are assumed to be susceptible. At any time t, the total population is given by $N(t) = S(t) + E(t) + I(t) + Q(t) + T(t) + R(t)$.

We consider the following system of non-linear differential equations for our model:

$$
\begin{cases}
\dfrac{dS(t)}{dt} = \Lambda - dS - \beta IS, \\
\dfrac{dE(t)}{dt} = \beta IS - (d+\alpha)E, \\
\dfrac{dI(t)}{dt} = \alpha E - (d+\lambda)I, \\
\dfrac{dQ(t)}{dt} = \lambda I - (d+h+\gamma)Q, \\
\dfrac{dT(t)}{dt} = hQ - (d+\delta+\rho)T, \\
\dfrac{dR(t)}{dt} = \gamma Q + \rho T - dR,
\end{cases} \tag{2.1}
$$

with initial conditions

$$
S(0) \geq 0, E(0) \geq 0, I(0) \geq 0, Q(0) \geq 0, T(0) \geq 0, R(0) \geq 0. \tag{2.2}
$$

Here, Λ is the birth rate, d is the natural death rate, β represents the effective contact rate of susceptible population with the infected population, α represents the proportion of exposed class who become infective, λ is the rate of quarantine, h is the rate at which people are being treated, γ is the recovery rate of a quarantined individual, δ represents the disease-induced death rate, and ρ represents the recovery rate due to treatment.

The diagrammatic representation of the mathematical model (1) is shown in Figure 1.

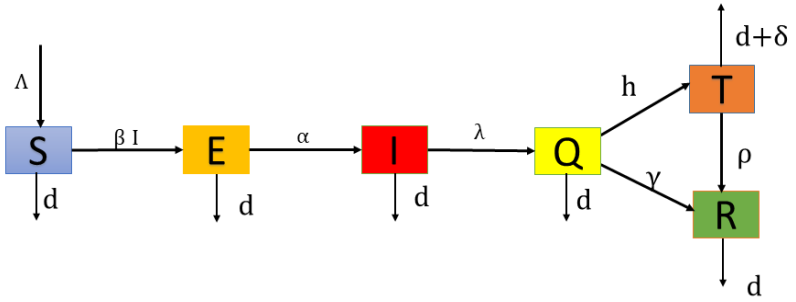

FIGURE 1. Graphical representation of the model (2.1).

3. BASIC PROPERTIES OF THE MODEL

By the fundamental theory of differential equations [66, 67], the solution of the system (2.1) with the initial conditions (2.2) exists for all $t \geq 0$ and it is unique. For the model to be realistic, the solutions must be non-negative and uniformly bounded. We check for that in this section.

3.1. Positivity of solutions.

Theorem 3.1. *If all the parameters are positive, then under initial conditions (2.2), the solutions of the system of equation (2.1), viz., $S(t), E(t), I(t), Q(t), T(t)$, and $R(t)$ are all non-negative for all $t \geq 0$.*

Proof. From the first equation of the system (2.1), we have

$$\frac{dS(t)}{dt} + B(t)S(t) = \Lambda, \tag{3.1}$$

where

$$B(t) = d + \beta I(t).$$

Multiplying equation (3.1) by $e^{\int_0^t B(s)ds}$, we get

$$\frac{dS(t)}{dt} e^{\int_0^t B(s)ds} + B(t)S(t)e^{\int_0^t B(s)ds} = \Lambda e^{\int_0^t B(s)ds}.$$

This implies that

$$\frac{d}{dt}(S(t)e^{\int_0^t B(s)ds}) = \Lambda e^{\int_0^t B(s)ds}. \tag{3.2}$$

Integrating equation (3.2) from 0 to t, we get

$$S(t)e^{\int_0^t B(s)ds} - S(0) = \Lambda \int_0^t e^{\int_0^u B(s)ds} du. \tag{3.3}$$

Multiplying equation (3.3) by $e^{-\int_0^t B(s)ds}$ gives us

$$S(t) = (S(0) + \Lambda \int_0^t e^{\int_0^u B(s)ds} du) \times e^{-\int_0^t B(s)ds}. \tag{3.4}$$

As every parameter is positive, equation (3.4) implies $\forall t \geq 0$,

$$S(t) \geq S(0)e^{-\int_0^t B(s)ds}. \tag{3.5}$$

As $S(0) \geq 0$ by (2.2), we conclude from equation (3.5) that $S(t)$ is positive for all $t > 0$.

Similarly, from the other equations of the system (2.1), we find

$$E(t) \geq E(0)e^{-(d+\alpha)t} \geq 0, \tag{3.6}$$

$$I(t) \geq I(0)e^{-(d+\lambda)t} \geq 0, \tag{3.7}$$

$$Q(t) \geq Q(0)e^{-(d+h+\gamma)t} \geq 0, \tag{3.8}$$

$$T(t) \geq T(0)e^{-(d+\delta+\rho)t} \geq 0, \tag{3.9}$$

$$R(t) \geq R(0)e^{-dt} \geq 0. \tag{3.10}$$

Thus, all the solutions $S(t), E(t), I(t), Q(t), T(t)$, and $R(t)$ of the system (2.1) are positive for all $t \geq 0$. This completes the proof of Theorem 1. □

3.2. Boundedness of solutions.

Theorem 3.2. *All feasible solutions $S(t), E(t), I(t), Q(t), T(t)$, and $R(t)$ of the system (2.1) are uniformly bounded on $[0, \infty)$.*

Proof. Adding all the equations of the model (2.1), we obtain

$$\frac{dN(t)}{dt} = \Lambda - dN(t) - \delta T(t). \tag{3.11}$$

Since $\delta > 0, T(t) \geq 0$, equation (3.11) implies

$$\frac{dN(t)}{dt} \leq \Lambda - dN(t). \tag{3.12}$$

Using Gronwall's inequality [73] for (3.12) we get

$$N(t) \leq \frac{\Lambda}{d} + (N(0) - \frac{\Lambda}{d})e^{-dt}, \tag{3.13}$$

for $t \geq 0$, $N(0)$ being the total initial population. Hence, $N(t) \leq \frac{\Lambda}{d}$ if $N(0) \leq \frac{\Lambda}{d}$. Therefore, if $N(0) \leq \frac{\Lambda}{d}$, the set defined by

$$\Omega = \left\{ (S, E, I, Q, T, R) \in \mathbb{R}^6_+ : N(t) \leq \frac{\Lambda}{d}, t \geq 0 \right\}, \tag{3.14}$$

is positively invariant and the solutions of the model (2.1) remain bounded. Further, equation (3.13) implies

$$\lim_{t \to +\infty} \sup N(t) \leq \frac{\Lambda}{d}. \tag{3.15}$$

From inequality (3.15), we have $N(t)$ approaches $\frac{\Lambda}{d}$ asymptotically for $N(0) > \frac{\Lambda}{d}$. Thus, all feasible solutions of the system (2.1) are uniformly bounded on $\mathbb{R}^6_+$. □

By virtue of Theorem 1 and Theorem 2, for the purpose of analyzing the model (2.1), it suffices to consider the region Ω as given by (3.14).

4. THE BASIC REPRODUCTION NUMBER R_0

The basic reproduction number R_0, is defined as the expected number of secondary cases that would arise from a typical primary case in a susceptible population [68, 69, 70, 71, 72]. We calculate the basic reproduction number from the first principle [70, 71]. On an average, an infected person remains infectious for a period of $1/(d+\lambda)$, the probability of the index case becoming infective rather than dying while in the class E is $\alpha/(\alpha+d)$ which will transmit infection at a rate $\beta \times \frac{\Lambda}{d}$, so the expected number of secondary cases caused by the index case in a completely susceptible population is: probability of making it through the latent stage without dying × rate of transmission while infectious × average infectious period. Thus,

$$R_0 = \frac{\alpha\beta\Lambda}{d(d+\alpha)(d+\lambda)}. \tag{4.1}$$

The effective reproduction number, given by $R_0 \times \frac{S(t)}{N(t)}$, is the expected number of secondary infection at time t[71].

5. STABILITY ANALYSIS OF THE MODEL

In this section, we find the steady-state solutions of the model and study their stability. We will see that the stability of the equilibria is intricately related to the value of R_0.

5.1. Equilibrium Points. We find the equilibrium points of the model by setting all the time derivatives in (2.1) to be zero. We see that there are two possible equilibria- one corresponding to having disease and the other one to no disease at all.

5.1.1. *The Disease Free Equilibrium.* The COVID-19 disease-free equilibrium DFE is obtained when there is no outbreak, i.e., $I = 0$. Solving the system (2.1) for $\dot{S} = \dot{E} = \dot{I} = \dot{Q} = \dot{T} =$

$\dot{R} = 0$ and $I = 0$ we get

$$DFE = (S^0, E^0, I^0, Q^0, T^0, R^0) = \left(\frac{\Lambda}{d}, 0, 0, 0, 0, 0\right). \tag{5.1}$$

5.1.2. *The Disease Present Equilibrium.* The COVID-19 disease present equilibrium DPE is obtained when there is an outbreak, i.e., $I \neq 0$. Solving the system (2.1) for $\dot{S} = \dot{E} = \dot{I} = \dot{Q} = \dot{T} = \dot{R} = 0$, and $I \neq 0$, we get

$$DPE = (S^*, E^*, I^*, Q^*, T^*, R^*), \tag{5.2}$$

where

$$\begin{cases} S^* = \dfrac{\Lambda}{dR_0}, \\ E^* = \dfrac{\Lambda}{d+\alpha}\dfrac{R_0-1}{R_0}, \\ I^* = \dfrac{\alpha\Lambda}{(d+\alpha)(d+\lambda)}\dfrac{R_0-1}{R_0}, \\ Q^* = \dfrac{\lambda\alpha\Lambda}{(d+\alpha)(d+\lambda)(d+h+\gamma)}\dfrac{R_0-1}{R_0}, \\ T^* = \dfrac{h\lambda\alpha\Lambda}{(d+\alpha)(d+\lambda)(d+h+\gamma)(d+\delta+\rho)}\dfrac{R_0-1}{R_0}, \\ R^* = \dfrac{\lambda\alpha\Lambda}{d(d+\alpha)(d+\lambda)(d+h+\gamma)}\left(\gamma + \dfrac{\rho h}{d+\delta+\rho}\right)\dfrac{R_0-1}{R_0}. \end{cases} \tag{5.3}$$

Ergo, $DPE = (S^*, E^*, I^*, Q^*, T^*, R^*)$ satisfies:

$$\begin{cases} 0 = \Lambda - dS^* - \beta I^* S^*, \\ 0 = \beta I^* S^* - (d+\alpha)E^*, \\ 0 = \alpha E^* - (d+\lambda)I^*, \\ 0 = \lambda I^* - (d+h+\gamma)Q^*, \\ 0 = hQ^* - (d+\delta+\rho)T^*, \\ 0 = \gamma Q^* + \rho T^* - dR^*. \end{cases} \tag{5.4}$$

5.2. Local stability. We now proceed to study the local stability behavior of the COVID-19 disease-free equilibrium DFE and endemic equilibrium DPE derived in (5.1) and (5.2), respectively.

5.2.1. *Local stability of the disease-free equilibrium.*

Theorem 5.1. *The disease-free equilibrium DFE as given by (5.1) is locally asymptotically stable if* $R_0 < 1$ *and unstable if* $R_0 > 1$.

Proof. This result is an immediate consequence of Theorem 2 in [69]. □

5.2.2. *Local stability of the disease-present equilibrium.*

Theorem 5.2. *The endemic equilibrium DPE is locally asymptotically stable if* $R_0 > 1$*, and unstable if* $R_0 < 1$.

Proof. The result is followed by an application of Theorem 4 in [69]. □

5.3. Global stability. We now move on to examine the global stability of the disease-free equilibrium DFE and endemic equilibrium DPE given by (5.1) and (5.2), respectively. In order to show that the system (2.1) is globally asymptotically stable, we shall make use of the Lyapunov second method and LaSalle's principle.

5.3.1. *Global stability of the COVID-19 disease-free equilibrium.*

Theorem 5.3. *The disease-free equilibrium DFE as given by (5.1) of system (2.1) is globally asymptotically stable in* Ω *if* $R_0 \leq 1$.

Proof. Consider the following Lyapunov function:

$$V(X(t)) = E(t) + \frac{S^0\beta}{d+\lambda} I(t), \tag{5.5}$$

where $X(t) = (S(t), E(t), I(t), Q(t), T(t), R(t))$ and $S^0 = \frac{\Lambda}{d}$ as obtained in (5.1). The function V satisfies:

$$\begin{cases} V(DFE) = 0, \\ V(X(t)) > 0, \text{ for all } X(t) \neq DFE, \text{ and} \\ V(X(t)) \text{ is radially unbounded: } V(X(t)) \to \infty \text{ as } \|X\| \to \infty. \end{cases} \tag{5.6}$$

Now, taking the time derivative of V along the trajectory of the model (2.1) in the region (3.14) we get,

$$\begin{aligned}
\frac{dV(X(t))}{dt} &= \dot{E(t)} + \frac{S^0\beta}{d+\lambda}\dot{I(t)} \\
&= \beta I(t)S(t) - (d+\alpha)E(t) + \frac{S^0\beta}{d+\lambda}(\alpha E(t) - (d+\lambda)I(t)) \\
&= \beta I(t)S(t) - (d+\alpha)E(t) + \frac{S^0\beta\alpha}{d+\lambda}E(t) - S^0\beta I(t) \\
&= \beta I(t)(S(t)-S^0) + (\alpha+d)(\frac{S^0\alpha\beta}{(\alpha+d)(d+\lambda)} - 1)E(t) \\
&= \beta I(t)(S(t)-S^0) + (\alpha+d)(R_0-1)E(t) \\
&\leq (d+\alpha)(R_0-1)E(t).
\end{aligned}$$

Therefore, $\frac{dV(X(t))}{dt} \leq 0$ for $R_0 \leq 1$, and $\frac{dV(X(t))}{dt} = 0$ iff $E = 0$ iff $I = 0$. This means that the set

$$V_{DFE} = \left\{ X(t) \in \Omega : \frac{dV(X(t))}{dt} = 0 \right\} = \{DFE\}, \tag{5.7}$$

is singleton containing the only point DFE obtained in (5.1). Hence, from Lasalle's invariance principle [74, 75, 76], the disease-free equilibrium DFE is globally asymptotically stable in Ω if $R_0 \leq 1$. □

5.3.2. *Global stability of the disease present equilibrium.* For the global stability of the endemic equilibrium, we use the following type of function:

$$f(x) = x - 1 - \ln x, \tag{5.8}$$

which is non-negative for $x > 0$, and $f(x) = 0$ iff $x = 1$. Besides,

$$f'(x) = 1 - 1/x. \tag{5.9}$$

We now present the final result on global stability.

Theorem 5.4. *The endemic equilibrium point DPE of the system (2.1) given by (5.2) is globally asymptotically stable in* Ω *if* $R_0 > 1$.

Proof. We define the following Lyapunov function L :

$$L(X(t)) = S^* f(S/S^*) + E^* f(E/E^*) + \frac{\beta I^* S^*}{\alpha E^*} I^* f(I/I^*), \tag{5.10}$$

where $X(t) = (S(t), E(t), I(t), Q(t), T(t), R(t))$. The function L satisfies the conditions (5.6) at *DPE*. Taking the time derivative of L along the trajectory of model (2.1) in the region (3.14), we get

$$\frac{dL(X(t))}{dt} = f'(S/S^*)S\dot{(t)} + f'(E/E^*)E\dot{(t)} + \frac{\beta I^* S^*}{\alpha E^*} f'(I/I^*)I\dot{(t)}. \tag{5.11}$$

Replacing the derivatives in the expression (5.11) using (2.1) and (5.9), we get

$$\begin{aligned} \dot{L}(X(t)) = &\left(1 - \frac{S^*}{S(t)}\right)(\Lambda - dS(t) - \beta I(t)S(t)) \\ &+ \left(1 - \frac{E^*}{E(t)}\right)(\beta I(t)S(t) - (d+\alpha)E(t)) \\ &+ \frac{\beta I^* S^*}{\alpha E^*}\left(1 - \frac{I^*}{I(t)}\right)(\alpha E(t) - (d+\lambda)I(t)) \end{aligned} \tag{5.12}$$

From (5.4), we get

$$\Lambda = dS^* + \beta I^* S^*, \qquad (d+\alpha) = \frac{\beta I^* S^*}{E^*}, \qquad (d+\lambda) = \frac{\alpha E^*}{I^*}. \tag{5.13}$$

Substituting (5.13) in (5.12), and regrouping the terms, we get

$$\dot{L}(X(t)) = -\frac{d\left(S(t) - S^*\right)^2}{S(t)} + \beta I^* S^* \left(3 - \frac{S^*}{S(t)} - \frac{E^* I(t) S(t)}{E(t) I^* S^*} - \frac{I^* E(t)}{I(t) E^*}\right). \tag{5.14}$$

Since $AM \geq GM$, we have

$$3 - \frac{S^*}{S(t)} - \frac{E^* I(t) S(t)}{E(t) I^* S^*} - \frac{I^* E(t)}{I(t) E^*} \leq 0.$$

Therefore, from (5.14)

$$\dot{L}(X(t)) \leq -\frac{d\left(S(t) - S^*\right)^2}{S(t)} \leq 0.$$

Moreover, for $R_0 > 1, \dot{L}(X(t)) = 0$ iff $X(t) = (S^*, E^*, I^*, Q^*, T^*, R^*)$. This implies that the set-

$$L_{DPE} = \left\{X(t) \in \Omega : \dot{L}(X(t)) = 0\right\} = \{DPE\}, \tag{5.15}$$

is singleton containing the only point *DPE* obtained in (5.3). Hence, from Lasalle's invariance principle [74, 75, 76], the endemic equilibrium *DPE* is globally asymptotically stable in Ω if $R_0 > 1$. □

6. BIFURCATION ANALYSIS

We observe that there is an exchange of stability between the disease free equilibrium DFE (5.1) and the disease present equilibrium DPE (5.2) when R_0 crosses the threshold value 1. So, the system (2.1) passes through a bifurcation at $R_0 = 1$. This is the subject of our ensuing theorem.

Theorem 6.1. *At $R_0 = 1$, the system (2.1) undergoes a transcritical bifurcation around its disease-free equilibrium.*

Proof. From stability analysis in Section 5, we have found that if $R_0 < 1$,only the disease-free equilibrium DFE(5.1) exists, and is stable both locally and globally. Further, if $R_0 > 1$, the disease prsesnt equilibrium DPE(5.2) arises and it is locally as well as globally asymptotically stable. Moreover, even though the disease-free equilibrium DFE(5.1) continues to exist for $R_0 > 1$, it is unstable. Thus, at the threshold $R_0 = 1$, there is a change in both feasibility and stability of system (2.1). Following the study in [78, 77, 79, 80, 81], we therefore come to the conclusion that at $R_0 = 1$, the system (2.1) undergoes a transcritical bifurcation. □

We graphically depict the bifurcation diagram of the system (2.1) in Figure 2.

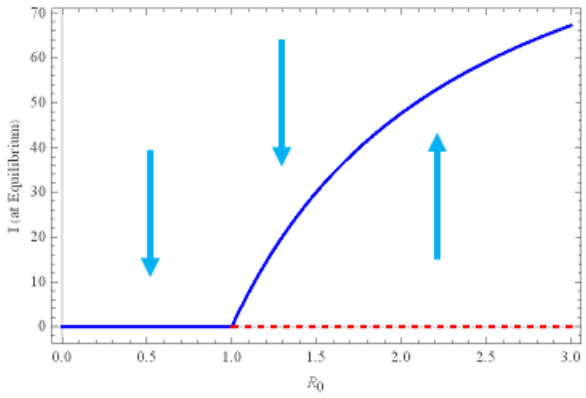

FIGURE 2. Forward transcritical bifurcation at $R_0 = 1$.

7. SENSITIVITY ANALYSIS OF R_0

Sensitivity analysis measures the relative change in a state variable with the change of a parameter. The normalized forward sensitivity index of a variable to a parameter is the ratio of the relative change in the variable to the relative change in the parameter.

Following Chitnis et al. [82], we calculate the normalized forward sensitivity indices of R_0. This will allow us to look at the relative impact of the parameters on the reproduction number R_0.

Let

$$\Upsilon_p^{R_0} = \frac{\partial R_0}{\partial p} \times \frac{p}{R_0},$$

denotes the sensitivity index of R_0 with respect to the parameter p.

From (4.1) we have

$$R_0 = \frac{\alpha\beta\Lambda}{d(d+\alpha)(d+\lambda)}.$$

Therefore,

$$\Upsilon_\beta^{R_0} = 1,$$

$$\Upsilon_\Lambda^{R_0} = 1,$$

$$\Upsilon_\rho^{R_0} = 0,$$

$$\Upsilon_\delta^{R_0} = 0,$$

$$\Upsilon_\alpha^{R_0} = \frac{d}{d+\alpha},$$

$$\Upsilon_\lambda^{R_0} = -\frac{\lambda}{d+\lambda},$$

$$\Upsilon_h^{R_0} = \Upsilon_\gamma^{R_0} = 0,$$

$$\Upsilon_d^{R_0} = -1 - \frac{d}{d+\alpha} - \frac{d}{d+\lambda}.$$

From above, we see that R_0, the basic reproduction number has a positive correlation with Λ, β, and α. This means that an increase or decrease in either of them will bring about a corresponding increase or decrease in the value of R_0. This is sensible since an increase in the birth rate or effective contact rate will increase the expected number of infected cases. Moreover, the sensitivity index of R_0 with respect to Λ and β is 1; which means that the change in the value of R_0 will be directly proportional to that of Λ and of β.

Parameter	Description	Sensitivity index
β	Effective contact rate	$+1$
Λ	Birth rate	$+1$
α	Proportion of exposed class who become infective	$+0.98$
ρ	Recovery rate due to treatment	0
δ	Disease induced death rate	0
d	Natural death rate	-2.09
γ	Recovery rate of quarantined individual	0
h	Treatment rate	0
λ	Quarantine rate	-0.88

TABLE 1. Sensitivity indices for different parameters of model (2.1).

Since people in the Q, T, or R compartment do not spread the disease, we observe that R_0 has no sensitivity towards quarantine individual's recovery rate γ, treatment rate h, and recovery due to treatment ρ. Similarly, λ and d have negative correlation with R_0. Hence, an increase in any one of them will bring about a decrease in R_0. This makes sense since, for example, an increase in the rate of quarantine will decrease the number of individuals spreading disease, and hence the expected number of infected cases. Thus, the sensitivity analysis of R_0 suggests that increasing the isolation or quarantine rate λ is a good way to reduce the disease spread.

We have shown the PRCC diagram of our model (2.1) in Figure 3.

8. NUMERICAL SIMULATIONS

We illustrate our theoretical results via numerical simulations in this section. We will use the Runge Kutta RK4 method to solve the initial value problem. We shall modify the initial values for the populations in various compartments of the model in order to corroborate our results on local and global stability. In each case, the total initial population is calculated by $N(0) = S(0) + E(0) + I(0) + Q(0) + T(0) + R(0)$. To substantiate the dependence of stability on the value of R_0, we use three different sets of parameters value so that $R_0 < 1$, $R_0 = 1$, and $R_0 > 1$, respectively.

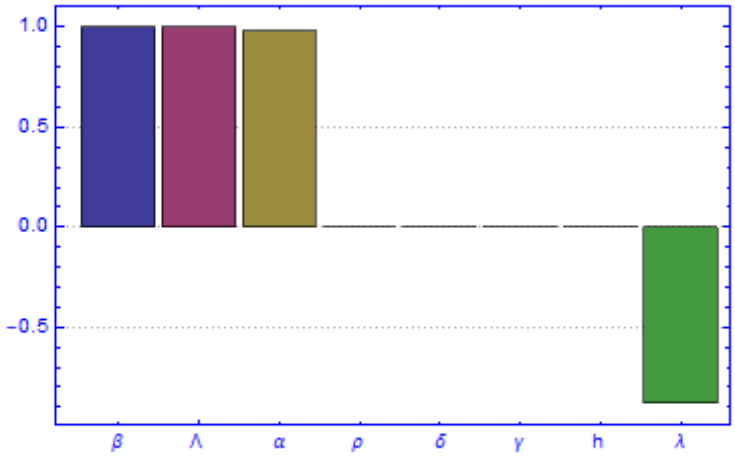

FIGURE 3. Sensitivity index of R_0 with respect to the parameters.

We present the first set of numerical simulation by using parameter value $\Lambda = 2000, \beta = 0.005, \alpha = 0.01, \lambda = 0.3, \rho = 0.25, \delta = 0.25, d = 0.4, h = 0.05$, and $\gamma = 0.10$. For these values of parameters, $R_0 = 0.871$ and the disease-free equilibrium is $DFE = (5000, 0, 0, 0, 0, 0)$. Since $R_0 < 1$, by Theorem 5, DFE is globally asymptotically stable. In this case, we see from Figure 4 that for any initial sub-population, the final susceptible population reaches the value 500 asymptotically, while the other classes *viz.*, exposed, infective, quarantined, recovered, and under-treatment class approaches zero; thus verifying Theorem 5.

For the next set of numerical simulations, we use the parameter value $\Lambda = 200$, $\beta = 0.005$, $\alpha = 0.1$, $\rho = 0.25$, $\lambda = 0.1$, $\delta = 0.25$, $d = 0.4$, $h = 0.05$, and $\gamma = 0.10$. In this case, $R_0 = 1$, and the disease-free equilibrium is $DFE = (500, 0, 0, 0, 0, 0)$. Since $R_0 = 1$, by Theorem 5, DFE is globally asymptotically stable. In fact, we see from Figure 5 that the final susceptible population approaches the value 500 asymptotically for any initial sub-population, while the other classes *viz.*, exposed, infectious, quarantined, recovered, and under-treatment class converge to zero. This confirms Theorem 5.

For the final case, we set the parameter values $\Lambda = 500$, $\beta = 0.002$, $\alpha = 0.001$, $\rho = 0.25$, $\delta = 0.25$, $d = 0.04$, $h = 0.3$, $\lambda = 0.05$, and $\gamma = 0.15$. In this case, $R_0 = 6.78$, and the endemic equilibrium is given by $DPE = (1845, 10395, 116, 12, 7, 85)$. Since $R_0 > 1$, by Theorem 6, DPE is globally asymptotically stable. Indeed, from Figure 6, the state variables approach their respective endemic steady state; establishing Theorem 6.

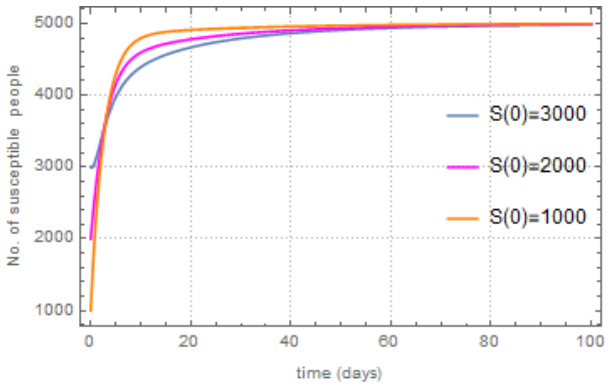

(A) Susceptible population

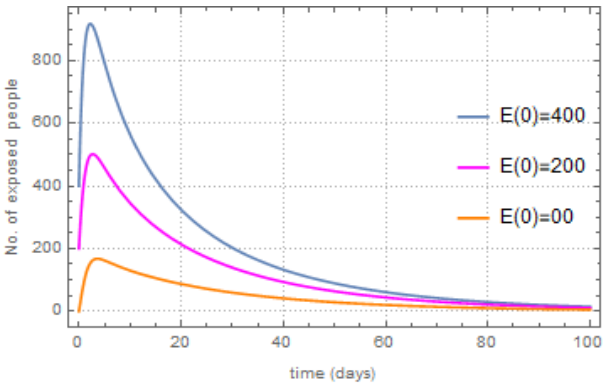

(B) Exposed population

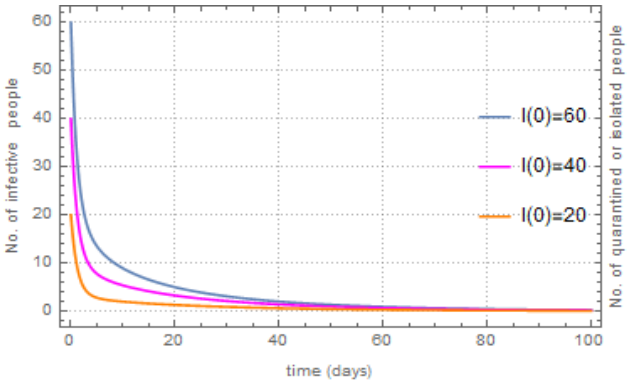

(C) Infective population

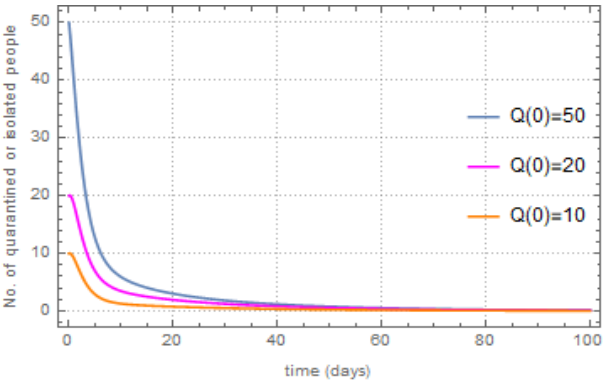

(D) Isolated or quarantine individuals

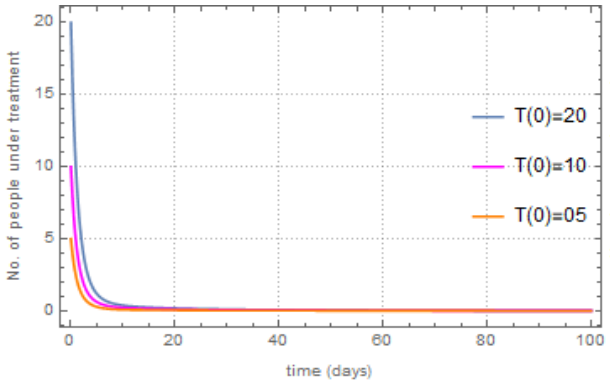

(E) Under-treatment population

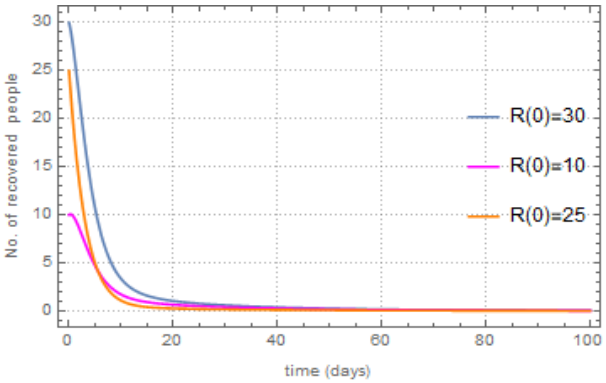

(F) Recovered population

FIGURE 4. Numerical simulation of model (2.1) for $R_0 < 1$. The system approaches the disease-free equilibrium point $DFE = (5000, 0, 0, 0, 0, 0)$ asymptotically.

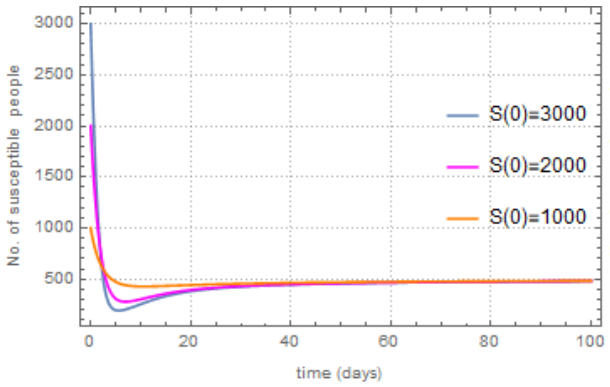

(A) Susceptible population

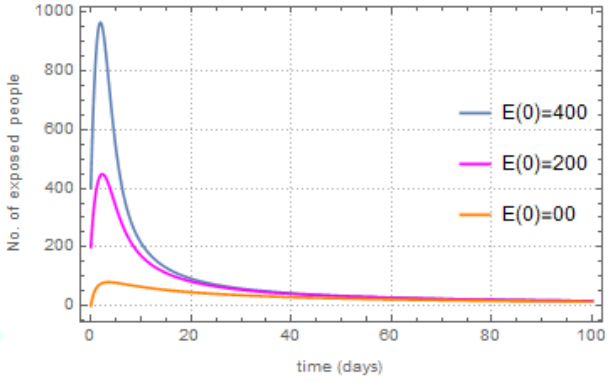

(B) Exposed population

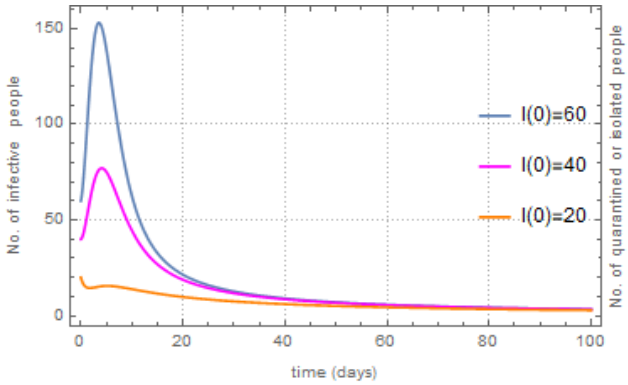

(C) Infective population

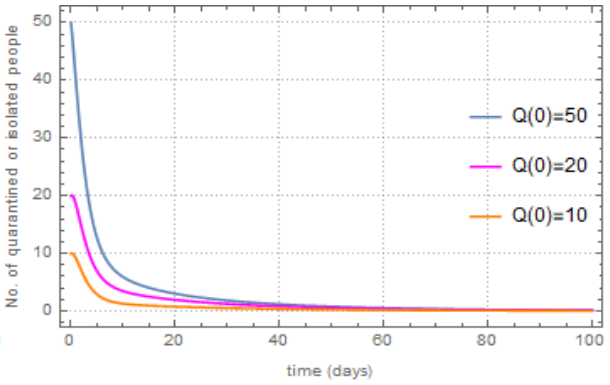

(D) Isolated or quarantine individuals

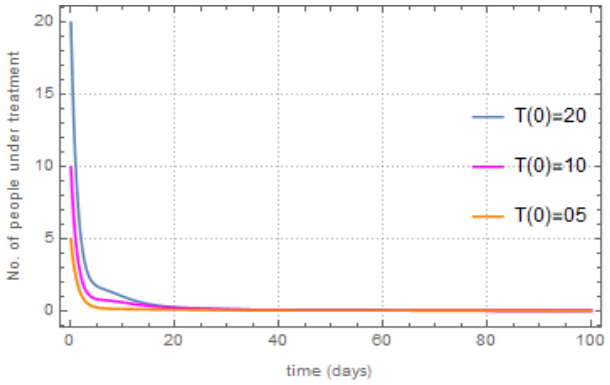

(E) Under-treatment population

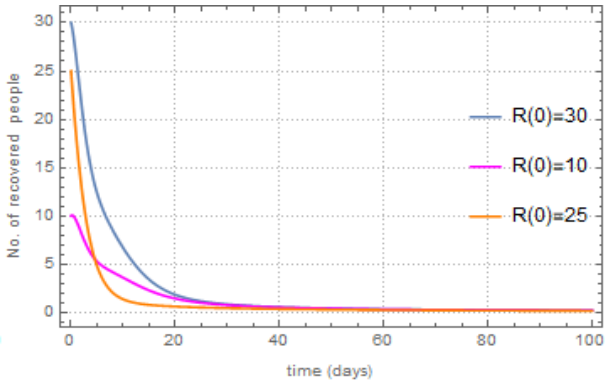

(F) Recovered population

FIGURE 5. Numerical simulation of model (2.1) for $R_0 = 1$. The system approaches the disease-free equilibrium $DFE = (500, 0, 0, 0, 0, 0)$ asymptotically.

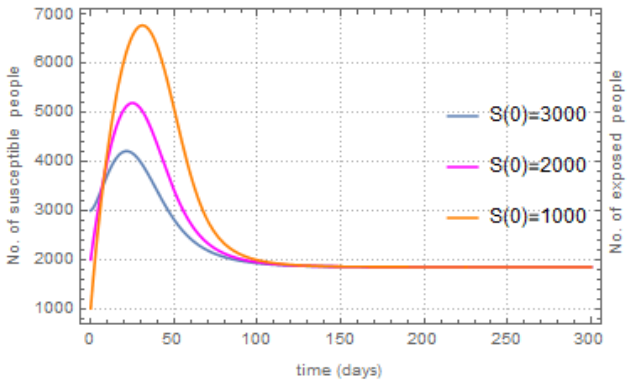

(A) Susceptible population

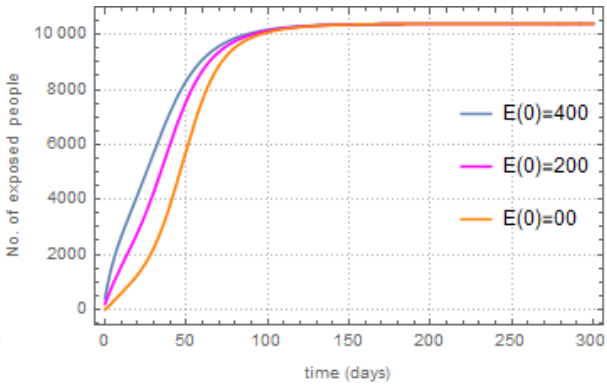

(B) Exposed population

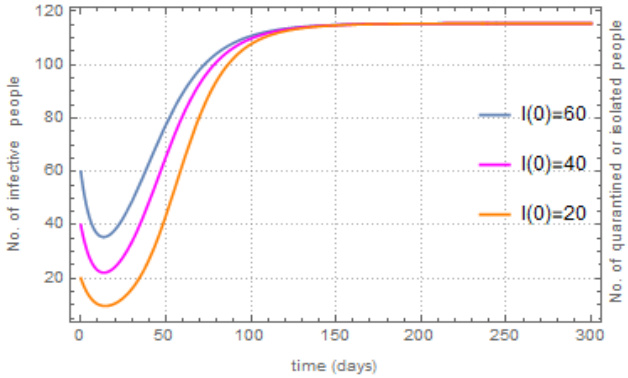

(C) Infective population

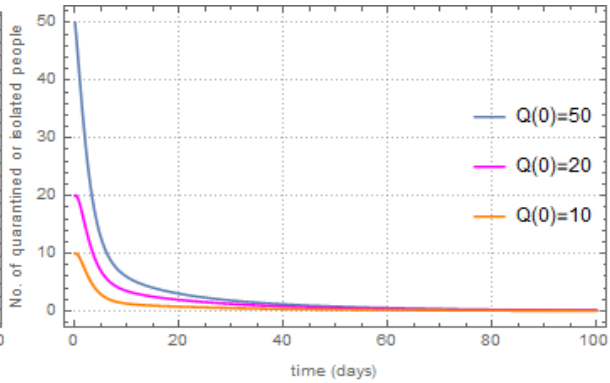

(D) Isolated or quarantine individuals

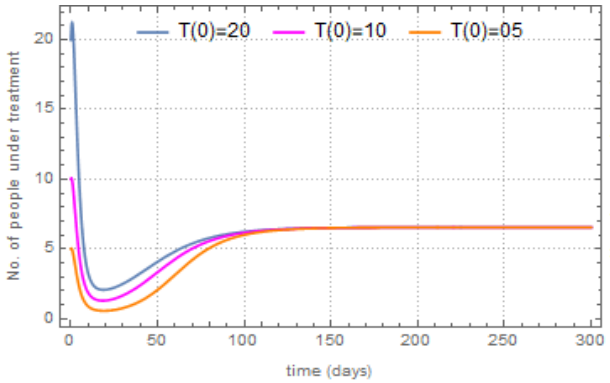

(E) Under-treatment population

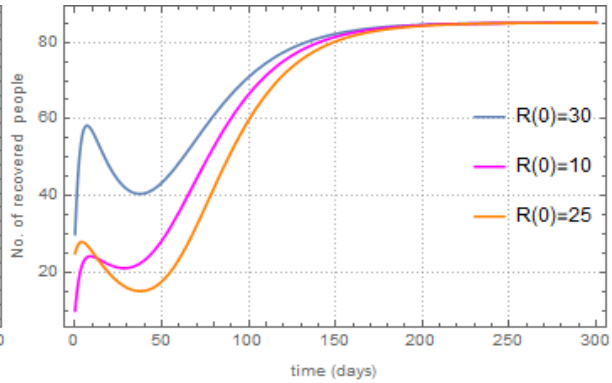

(F) Recovered population

FIGURE 6. Numerical simulation of model (2.1) for $R_0 > 1$. The system approaches the endemic equilibrium point $DPE = (1845, 10395, 116, 12, 7, 85)$ asymptotically.

9. Discussions and Conclusions

In this paper, we have formulated a continuous-time mathematical model for the COVID-19 disease spread, described by a system of ordinary differential equations. We have studied the basic properties of the model (2.1) *viz.*, positivity and boundedness. The basic reproduction number has been derived to be $R_0 = \frac{\alpha\beta\Lambda}{d(d+\alpha)(d+h+\gamma)}$, and its relation to the stability of the model dynamics has been established. We calculated the equilibria of the model and found that the disease-free equilibrium is locally stable for $R_0 \leq 1$, while the endemic equilibrium is locally stable for $R_0 > 1$. We also established that there is a unique globally stable disease-free equilibrium when $R_0 \leq 1$, and a unique globally stable disease-present equilibrium when $R_0 > 1$. The global stability of the two equilibria has been proved by considering a suitable Lyapunov functional for the respective cases and invoking the LaSalle invariant principle. In order to see the impact of parameters on the spread dynamics of the disease, we performed sensitivity analysis of the basic reproduction number R_0. Finally, we demonstrated our theoretical findings with the help of some numerical simulations carried out under different initial conditions.

From the overall study, it is found that the transmission of COVID-19 can be controlled by maintaining the value of basic reproduction number less than or equal to one, which can be done by manipulating different model parameters. In this regard, the sensitivity analysis indicates that the transmission of COVID-19 can be lowered by increasing the rate of quarantine. Thus the quarantining of infected population plays a crucial rule to control the transmission of COVID-19. However, there are some drawbacks in this model, for example: the immunity is assumed for lifelong once recovered, which needs further research. But, it is expected that the qualitative behavior of the model will be unchanged by this. In addition, vaccination has not been considered. We plan to incorporate these in our future work.

Conflict of Interests

The author(s) declare that there is no conflict of interests.

References

[1] World Health Organisation, https://www.who.int/emergencies/diseases/novel-coronavirus-2019/situation-reports/.

[2] Johns Hopkins University and Medicine, (2020). https://coronavirus.jhu.edu.

[3] Centers for Disease Control and Prevention, (2020). https://www.cdc.gov/coronavirus/2019-nCoV/index.html.

[4] T.H.E. Alves, T.A. de Souza, S. de A. Silva, et al. Underreporting of death by COVID-19 in Brazil's second most populous state, Front. Public Health. 8 (2020), 578645. https://doi.org/10.3389/fpubh.2020.578645.

[5] S. Arvisais-Anhalt, C.U. Lehmann, J.Y. Park, et al. What the coronavirus disease 2019 (COVID-19) pandemic has reinforced: the need for accurate data, Clinic. Infect. Dis. 72 (2020), 920–923. https://doi.org/10.1093/cid/ciaa1686.

[6] A. Azmon, C. Faes, N. Hens, On the estimation of the reproduction number based on misreported epidemic data, Stat. Med. 33 (2013), 1176–1192. https://doi.org/10.1002/sim.6015.

[7] T. Burki, COVID-19 in Latin America, Lancet Infect. Dis. 20 (2020), 547–548. https://doi.org/10.1016/s1473-3099(20)30303-0.

[8] M.F. do Prado, B.B. de P. Antunes, L. dos S.L. Bastos, et al. Analysis of COVID-19 under-reporting in Brazil, Rev. Brasil. Terapia Intensiva. 32 (2020), 224–228. https://doi.org/10.5935/0103-507x.20200030.

[9] H. Lau, T. Khosrawipour, P. Kocbach, et al. Evaluating the massive underreporting and undertesting of COVID-19 cases in multiple global epicenters, Pulmonology. 27 (2021), 110–115. https://doi.org/10.1016/j.pulmoe.2020.05.015.

[10] Z.E. Rasjid, R. Setiawan, A. Effendi, A Comparison: Prediction of death and infected COVID-19 cases in Indonesia using time series smoothing and LSTM neural network, Procedia Computer Sci. 179 (2021), 982–988. https://doi.org/10.1016/j.procs.2021.01.102.

[11] M. Saberi, H. Hamedmoghadam, K. Madani, et al. Accounting for underreporting in mathematical modeling of transmission and control of COVID-19 in Iran, Front. Phys. 8 (2020), 00289. https://doi.org/10.3389/fphy.2020.00289.

[12] A.J.Q. Sarnaglia, B. Zamprogno, F.A. Fajardo Molinares, et al. Correcting notification delay and forecasting of COVID-19 data, J. Math. Anal. Appl. 514 (2022), 125202. https://doi.org/10.1016/j.jmaa.2021.125202.

[13] M. Worobey, J.I. Levy, L. Malpica Serrano, et al. The Huanan Seafood Wholesale Market in Wuhan was the early epicenter of the COVID-19 pandemic, Science. 377 (2022), 951–959. https://doi.org/10.1126/science.abp8715.

[14] P. Zhou, X.L. Yang, X.G. Wang, et al. A pneumonia outbreak associated with a new coronavirus of probable bat origin, Nature. 579 (2020), 270–273. https://doi.org/10.1038/s41586-020-2012-7.

[15] A. Maxmen, Wuhan market was epicentre of pandemic's start, studies suggest, Nature. 603 (2022), 15–16. https://doi.org/10.1038/d41586-022-00584-8.

[16] G. Gao, W. Liu, P. Liu, et al. Surveillance of SARS-CoV-2 in the environment and animal samples of the Huanan Seafood Market, (2022). https://doi.org/10.21203/rs.3.rs-1370392/v1.

[17] J.E. Pekar, A. Magee, E. Parker, et al. SARS-CoV-2 emergence very likely resulted from at least two zoonotic events, (2022). https://doi.org/10.5281/ZENODO.6291628.

[18] G. Chowell, C. Castillo-Chavez, P.W. Fenimore, et al. Model parameters and outbreak control for SARS, Emerg. Infect. Dis. 10 (2004), 1258–1263. https://doi.org/10.3201/eid1007.030647.

[19] M. Kretzschmar, J. Wallinga, Mathematical Models in Infectious Disease Epidemiology, in: A. Kramer, M. Kretzschmar, K. Krickeberg (Eds.), Modern Infectious Disease Epidemiology, Springer New York, 2009: 209—221.

[20] S. Sharma, G.P. Samanta, Stability analysis and optimal control of an epidemic model with vaccination, Int. J. Biomath. 08 (2015), 1550030. https://doi.org/10.1142/s1793524515500308.

[21] S.A. Levin, New Directions in the Mathematics of Infectious Disease, in: C. Castillo-Chavez, S. Blower, P. van den Driessche, D. Kirschner, A.-A. Yakubu (Eds.), Mathematical Approaches for Emerging and Reemerging Infectious Diseases: Models, Methods, and Theory, Springer New York, 2002: 1—5.

[22] H.W. Hethcote, The mathematics of infectious diseases, SIAM Rev. 42 (2000), 599–653. https://doi.org/10.1137/s0036144500371907.

[23] [1] F. Brauer, C. Castillo-Chavez, Mathematical Models in Population Biology and Epidemiology, Springer New York, New York, NY, 2012. https://doi.org/10.1007/978-1-4614-1686-9.

[24] W.O. Kermack, A.G. McKendrick, A contribution to the mathematical theory of epidemics, Proc. R. Soc. Lond. A. 115 (1927), 700–721. https://doi.org/10.1098/rspa.1927.0118.

[25] N.T.J. Bailey, The mathematical theory of epidemics, Griffin, London, (1957).

[26] M.S. Bartlett, Stochastic population models in ecology and epidemiology, Wiley, New York, (1960).

[27] M. Bartlett, Deterministic and stochastic models for recurrent epidemics, In: Proceedings of the Third Berkeley Symposium on Mathematical Statistics and Probability, 4 (1956), 81–109.

[28] M.S. Bartlett, The critical community size for measles in the United States, J. R. Stat. Soc. Ser. A. 123 (1960), 37–44. https://doi.org/10.2307/2343186.

[29] J.K. K. Asamoah, C.S. Bornaa, B. Seidu, et al. Mathematical analysis of the effects of controls on transmission dynamics of SARS-CoV-2, Alexandria Eng. J. 59 (2020), 5069–5078. https://doi.org/10.1016/j.aej.2020.09.033.

[30] Y. Hao, T. Xu, H. Hu, et al. Prediction and analysis of Corona Virus Disease 2019, PLoS ONE. 15 (2020), e0239960. https://doi.org/10.1371/journal.pone.0239960.

[31] S.M. Kassa, J.B.H. Njagarah, Y.A. Terefe, Analysis of the mitigation strategies for COVID-19: From mathematical modelling perspective, Chaos Solitons Fractals. 138 (2020), 109968. https://doi.org/10.1016/j.chaos.2020.109968.

[32] A.J. Kucharski, T.W. Russell, C. Diamond, et al. Early dynamics of transmission and control of COVID-19: a mathematical modelling study, Lancet Infect. Dis. 20 (2020), 553–558. https://doi.org/10.1016/s1473-3099(20)30144-4.

[33] T. Zhou, Q. Liu, Z. Yang, et al. Preliminary prediction of the basic reproduction number of the Wuhan novel coronavirus 2019-nCoV, J. Evid. Based Med. 13 (2020), 3–7. https://doi.org/10.1111/jebm.12376.

[34] Q. Lin, S. Zhao, D. Gao, et al. A conceptual model for the coronavirus disease 2019 (COVID-19) outbreak in Wuhan, China with individual reaction and governmental action, Int. J. Infect. Dis. 93 (2020), 211–216. https://doi.org/10.1016/j.ijid.2020.02.058.

[35] B. Tang, F. Xia, S. Tang, et al. The effectiveness of quarantine and isolation determine the trend of the COVID-19 epidemics in the final phase of the current outbreak in China, Int. J. Infect. Dis. 95 (2020), 288–293. https://doi.org/10.1016/j.ijid.2020.03.018.

[36] C. Anastassopoulou, L. Russo, A. Tsakris, C. Siettos, Data-based analysis, modelling and forecasting of the COVID-19 outbreak, PLoS ONE. 15 (2020), e0230405. https://doi.org/10.1371/journal.pone.0230405.

[37] L. Lopez, X. Rodo, A modified SEIR model to predict the COVID-19 outbreak in Spain and Italy: Simulating control scenarios and multi-scale epidemics, Results Phys. 21 (2021), 103746. https://doi.org/10.1016/j.rinp.2020.103746.

[38] A. Radulescu, C. Williams, K. Cavanagh, Management strategies in a SEIR-type model of COVID 19 community spread, Sci. Rep. 10 (2020), 21256. https://doi.org/10.1038/s41598-020-77628-4.

[39] M. Batista, Estimation of the final size of the COVID-19 epidemic, medRxiv (2020). https://doi.org/10.1101/2020.02.16.20023606.

[40] Z. Bai, Y. Gong, X. Tian, et al. The rapid assessment and early warning models for COVID-19, Virol. Sin. 35 (2020), 272–279. https://doi.org/10.1007/s12250-020-00219-0.

[41] X. Liu, G.J.D. Hewings, M. Qin, et al. Modelling the situation of COVID-19 and effects of different containment strategies in China with dynamic differential equations and parameters estimation, SSRN. (2020). https://doi.org/10.2139/ssrn.3551359.

[42] J. Jia, J. Ding, S. Liu, et al. Modeling the control of COVID-19: impact of policy interventions and meteorological factors, (2020). http://arxiv.org/abs/2003.02985.

[43] Z. Liu, P. Magal, O. Seydi, G. Webb, Predicting the cumulative number of cases for the COVID-19 epidemic in China from early data, Math. Biosci. Eng. 17 (2020), 3040–3051. https://doi.org/10.3934/mbe.2020172.

[44] S.B. Bastos, D.O. Cajueiro, Modeling and forecasting the early evolution of the Covid-19 pandemic in Brazil, Sci. Rep. 10 (2020), 19457. https://doi.org/10.1038/s41598-020-76257-1.

[45] S. Pengpeng, C. Shengli, F. Peihua, SEIR Transmission dynamics model of 2019 nCoV coronavirus with considering the weak infectious ability and changes in latency duration, medRxiv (2020). https://doi.org/10.1101/2020.02.16.20023655.

[46] C. Tsay, F. Lejarza, M.A. Stadtherr, et al. Modeling, state estimation, and optimal control for the US COVID-19 outbreak, Sci. Rep. 10 (2020), 10711. https://doi.org/10.1038/s41598-020-67459-8.

[47] C. Hou, J. Chen, Y. Zhou, et al. The effectiveness of quarantine of Wuhan city against the Corona Virus Disease 2019 (COVID-19): A well-mixed SEIR model analysis, J. Med. Virol. 92 (2020), 841–848. https://doi.org/10.1002/jmv.25827.

[48] J. Cao, X. Jiang, B. Zhao, et al. Mathematical modeling and epidemic prediction of covid-19 and its significance to epidemic prevention and control measures, J. Biomed. Res. Innov. 1 (2020), 103.

[49] A. Senapati, S. Rana, T. Das, et al. Impact of intervention on the spread of COVID-19 in India: A model based study, J. Theor. Biol. 523 (2021), 110711. https://doi.org/10.1016/j.jtbi.2021.110711.

[50] B. Ivorra, M.R. Ferrandez, M. Vela-Perez, et al. Mathematical modeling of the spread of the coronavirus disease 2019 (COVID-19) taking into account the undetected infections. The case of China, Commun. Nonlinear Sci. Numer. Simul. 88 (2020), 105303. https://doi.org/10.1016/j.cnsns.2020.105303.

[51] A.N. Chatterjee, F. Al Basir, A model for SARS-CoV-2 infection with treatment, Comput. Math. Methods Med. 2020 (2020), 1352982. https://doi.org/10.1155/2020/1352982.

[52] S. Zhao, Q. Lin, J. Ran, et al. Preliminary estimation of the basic reproduction number of novel coronavirus (2019-nCoV) in China, from 2019 to 2020: A data-driven analysis in the early phase of the outbreak, Int. J. Infect. Dis. 92 (2020), 214–217. https://doi.org/10.1016/j.ijid.2020.01.050.

[53] M.S. Boudrioua, A. Boudrioua, Predicting the COVID-19 epidemic in Algeria using the SIR model, medRxiv (2020). https://doi.org/10.1101/2020.04.25.20079467.

[54] X. Zhou, X. Ma, N. Hong, et al. Forecasting the worldwide spread of COVID-19 based on logistic model and SEIR model, medRxiv (2020). https://doi.org/10.1101/2020.03.26.20044289.

[55] K. Liang, Mathematical model of infection kinetics and its analysis for COVID-19, SARS and MERS, Infect. Genetics Evol. 82 (2020), 104306. https://doi.org/10.1016/j.meegid.2020.104306.

[56] R.M. Anderson, B. Anderson, R.M. May, Infectious diseases of humans: dynamics and control, Oxford University Press, Oxford (1992).

[57] H.W. Hethcote, The mathematics of infectious diseases, SIAM Rev. 42 (2000), 599–653. https://doi.org/10.1137/s0036144500371907.

[58] F.B. Hamzah, C. Lau, H. Nazri, et al. Coronatracker: worldwide COVID-19 outbreak data analysis and prediction. Bull. World Health Organ. 1 (2020), 32.

[59] S. Clifford, C.A.B. Pearson, P. Klepac, et al. Effectiveness of interventions targeting air travellers for delaying local outbreaks of SARS-CoV-2, J. Travel Med. 27 (2020), taaa068. https://doi.org/10.1093/jtm/taaa068.

[60] B. Tang, N.L. Bragazzi, Q. Li, et al. An updated estimation of the risk of transmission of the novel coronavirus (2019-nCov), Infect. Dis. Model. 5 (2020), 248–255. https://doi.org/10.1016/j.idm.2020.02.001.

[61] B. Tang, X. Wang, Q. Li, et al. Estimation of the transmission risk of the 2019-nCoV and its implication for public health interventions, J. Clin. Med. 9 (2020), 462. https://doi.org/10.3390/jcm9020462.

[62] H. Xiong, H. Yan, Simulating the infected population and spread trend of 2019-ncov under different policy by EIR model, SSRN, (2020). https://ssrn.com/abstract=3537083.

[63] Y. Chen, J. Cheng, Y. Jiang, et al. A time delay dynamical model for outbreak of 2019-nCoV and the parameter identification, J. Inverse Ill-Posed Probl. 28 (2020), 243–250. https://doi.org/10.1515/jiip-2020-0010.

[64] R. Niu, E.W.M. Wong, Y.C. Chan, et al. Modeling the COVID-19 pandemic using an SEIHR model with human migration, IEEE Access. 8 (2020), 195503–195514. https://doi.org/10.1109/access.2020.3032584.

[65] O. Diekmann, J.A.P. Heesterbeek, Mathematical Epidemiology of Infectious Diseases: Model Building, Analysis and Interpretation, Wiley, New York, (2000).

[66] J.D. Lambert, Computational Methods in Ordinary Differential Equations, Wiley, New York, (1973).

[67] J.A.N. Fred Brauer, The Qualitative Theory of Ordinary Differential Equations: An Introduction, Dover Publications, New York, (1989).

[68] H.W. Hethcote, Mathematics of infectious diseases, SIAM Rev. 42 (2005), 599–653. https://www.jstor.org/stable/2653135.

[69] P. van den Driessche, J. Watmough, Reproduction numbers and sub-threshold endemic equilibria for compartmental models of disease transmission, Math. Biosci. 180 (2002), 29–48. https://doi.org/10.1016/s0025-5564(02)00108-6.

[70] O.N. Bjørnstad, Epidemics: models and data using R, Springer-Verlag, New York, (2018).

[71] O.N. Bjørnstad, K. Shea, M. Krzywinski, et al. The SEIRS model for infectious disease dynamics, Nat. Methods. 17 (2020), 557–558. https://doi.org/10.1038/s41592-020-0856-2.

[72] M.G. Roberts, J.A.P. Heesterbeek, A new method for estimating the effort required to control an infectious disease, Proc. R. Soc. Lond. B. 270 (2003), 1359–1364. https://doi.org/10.1098/rspb.2003.2339.

[73] S.S. Dragomir, Some Gronwall type inequalities and applications, (2002). https://rgmia.org/papers/monographs/standard.pdf.

[74] J.P. La Salle, The Stability of Dynamical Systems, Society for Industrial and Applied Mathematics, (1976).

[75] J. LaSalle, Some Extensions of Liapunov's second method, IRE Trans. Circuit Theory. 7 (1960), 520–527. https://doi.org/10.1109/tct.1960.1086720.

[76] J.K. Hale, S.M.V. Lunel, Introduction to Functional Differential Equations, Springer New York, 1993. https://doi.org/10.1007/978-1-4612-4342-7.

[77] J. Guckenheimer, P. Holmes, M. Slemrod, Nonlinear oscillations dynamical systems, and bifurcations of vector fields, J. Appl. Mech. 51 (1984), 947-947. https://doi.org/10.1115/1.3167759.

[78] J. Guckenheimer, H. Philip, Nonlinear oscillations, dynamical systems, and bifurcations of vector fields, Vol. 42, Springer, (2013).

[79] S. Jana, P. Haldar, T.K. Kar, Mathematical analysis of an epidemic model with isolation and optimal controls, Int. J. Computer Math. 94 (2016), 1318–1336. https://doi.org/10.1080/00207160.2016.1190009.

[80] T.K. Kar, S. Jana, A theoretical study on mathematical modelling of an infectious disease with application of optimal control, Biosystems. 111 (2013), 37–50. https://doi.org/10.1016/j.biosystems.2012.10.003.

[81] J. Dushoff, H. Wenzhang, C. Castillo-Chavez, Backwards bifurcations and catastrophe in simple models of fatal diseases, J. Math. Biol. 36 (1998), 227–248.

[82] N. Chitnis, J.M. Hyman, J.M. Cushing, Determining important parameters in the spread of malaria through the sensitivity analysis of a mathematical model, Bull. Math. Biol. 70 (2008), 1272–1296. https://doi.org/10.1007/s11538-008-9299-0.